SUPERCONDUCTING CRAB CAVITY OPTIONS FOR SHORT X-RAY PULSE GENERATION IN SPEAR3*

F. Toufexis†, V.A. Dolgashev, X. Huang, Z. Li, SLAC, Menlo Park, CA 94025

Abstract

We are exploring methods to generate short X-ray pulses in SPEAR3 on the order of 1 ps to enable studying ultrafast processes in materials. We are developing a 2-frequency crab cavity scheme with two sets of crab cavities at the 6th and 6.5th harmonics of the 476 MHz ring RF frequency. In previous work we studied a normal conducting crab cavity for SPEAR3. In this work we explored two superconducting cavity options: a traditional elliptical cavity and the Quasi-waveguide Resonator. We found that the Quasi-waveguide Resonator cannot meet our field uniformity specifications due to higher order multipole fields. We then optimized a traditional elliptical cavity with the input, Lower Order Modes, and Higher Order Modes couplers following the Argonne Advanced Photon Source design.

INTRODUCTION

Synchrotron Light Sources based on storage rings produce photon pulses on the order of 20 ps RMS [1, 2]. Developing short x-ray pulse capability in storage rings would enable several scientific applications including material research for efficient solar energy conversion [3–6], ultrafast optical control of structural dynamics, nanoscopic thermal transport & thermoelectrics [7], and the development of an incoherent time-resolved alternative to X-ray Photon Correlation Spectroscopy. These applications require a photon flux of more than 1×10^{12} ph/s [8].

There are several methods to enable short x-ray pulse capability in storage rings: low-alpha modes, pseudo single bunch operation [9], resonant crabbing [10], short pulse injection from the LCLS-II Superconducting (SC) linac [11, 12], single frequency crab cavities [13–18], longitudinal bunch compression using 2-frequency accelerating SC cavities [11, 19], and transverse bunch crabbing using 2-frequency crab cavities [11, 20] that is the focus of this paper.

In the 2-frequency crab cavity scheme there are two sets of crab cavities at the 6th and 6.5th harmonics of the ring RF frequency of 476 MHz. As these two frequencies beat, in half of the buckets the beam is left unaffected while in the other half it is tilted. A high charge so-called camshaft bunch is injected in one of the tilted buckets to generate a short X-ray pulse. A normal conducting crab cavity design has already been explored for SPEAR3 [20]. In this work we investigate a SC crab cavity alternative. We begin by reviewing the design requirements and then show optimization data for two different cavities: the elliptical and the single-cell Quasi-waveguide Multi-cell Resonator (QMiR) [21].

* This project was funded by U.S. Department of Energy under Contract No. DE-AC02-76SF00515.

† ftouf@slac.stanford.edu

DESIGN REQUIREMENTS

The design requirements for the crab cavity are summarized in Table 1. The SPEAR3 RF frequency is 476.314 MHz and the crab cavities will operate at the 6th and 6.5th harmonics. The wakefield-related requirements are identical to the warm two-frequency crab cavity system we previously explored [20]. The beam aperture throughout the cavities should be larger than 3.6 cm in the horizontal plane to accommodate for the large initial oscillations of the injected beam in the ring. One important requirement for SPEAR3 is the kick uniformity on the transverse plane, and specifically the maximum allowable magnitude of the sextupole component of the deflecting RF fields.

MULTIPOLE EXPANSION

For a non-axisymmetric cavity there will be a kick variation within the aperture $V(r,\phi) = V_d + \Delta V(r,\phi)$, where V_d is the nominal deflection at the beam axis, and r and ϕ are the transverse polar coordinates. To calculate the multipole components of the RF fields we fit on the relative transverse kick variation $\frac{\Delta V(r,\phi)}{V_d}$ in the azimuth for different radius the following expression: $\sum_{n=1}^{\infty} r^n \left[a_n \sin(n\phi) + b_n \cos(n\phi)\right]$, where the term $n = 1$ to the quadrupole component, $n = 2$ to the sextupole component, *etc*. We can write the kick variation due to the sextupole component $K_2 L/2 = \sqrt{a_2^2 + b_2^2}$ as $\frac{\Delta V(r,\phi)}{V_d} = \frac{E\sqrt{a_2^2+b_2^2}}{V_b} r^2$, where E is the beam energy 3 GeV. For our machine parameters we need $\frac{\Delta V(r,\phi)}{V_d} \leq 150 r^2$.

Table 1: Superconducting Crab Cavity Design Requirements, Adapted from Li *et al.* [20]

Parameter	Value
1st crab cavity frequency f_1	2.858 GHz
2nd crab cavity frequency f_2	3.096 GHz
1st crab cavity voltage V_1	1.0 MV
2nd crab cavity voltage V_2	0.93 MV
Beam aperture d	> 3.6 cm
Bunch kick factor k_d	$< 1500\,\mathrm{V\,pC^{-1}\,m^{-1}}$
Sextupole field $K_2 L$	$< 0.2\,\mathrm{m^{-2}}$
Long. wake impedance Z_n/n	$< 8.3\,\mathrm{k\Omega}$ @ 3 GHz
Trans. wake impedance Z_x	$< 4.7\,\mathrm{M\Omega\,m^{-1}}$
Trans. wake impedance Z_y	$< 1.9\,\mathrm{M\Omega\,m^{-1}}$

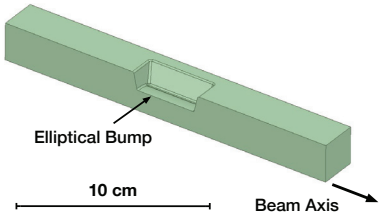

(a) Quarter of the single-cell QMiR geometry as simulated with HFSS.

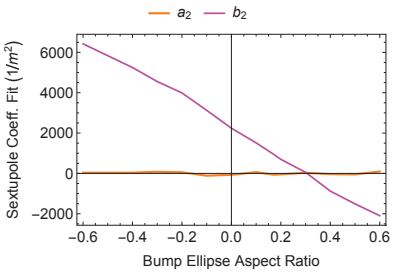

(b) Sextupole coefficients a_2 and b_2 versus ellipse shape.

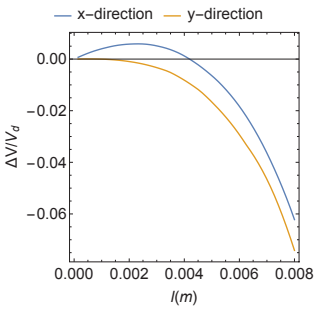

(c) Kick variation in x and y for bump ellipse aspect ratio 0.3.

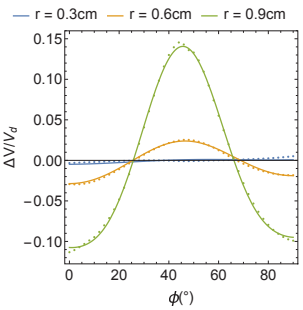

(d) Kick variation in the azimuth at different radius for bump ellipse aspect ratio 0.3. Dotted line is simulation data, solid line is multipole fit.

Figure 1: QMiR crab cavity optimization.

QUASI-WAVEGUIDE RESONATOR

The QMiR crab cavity shape was proposed for APS [21]. The single-cell QMiR cavity shown in Fig. 1a has a characteristic bump that traps a deflecting mode. This cavity has the advantage that the deflecting mode is the fundamental mode and therefore there are no Lower Order Modes (LOM), while Higher Order Modes (HOM) are dumped through the beam pipe. However, this shape has substantial sextupole and other high-order components, which are an issue for SPEAR3 operation. To cancel the sextupole component we made the bump profile elliptical. Fig. 1b shows the results of the optimization of the ellipse on the bump. At bump ellipse aspect ratio of 0.3 the sextupole component is minimized. Fig. 1c and Fig. 1d show the kick variation with x and y and azimuthally for different radius having multipole fields of order $n = 1, 2, 4, 8$. Although we have cancelled the sextupole coefficients a_2 and b_2, the higher order terms, especially the terms a_4 and b_4, are substantial as shown in Fig. 1d. We therefore concluded at this point that the QMiR crab cavity shape is not suitable for SPEAR3.

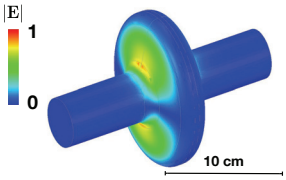

Figure 2: Elliptical crab cavity with optimized shape.

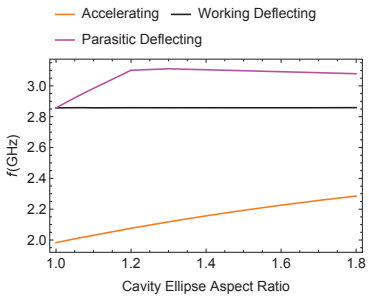

Figure 3: Accelerating and parasitic deflecting mode frequency versus cavity ellipse aspect ratio for constant working mode frequency.

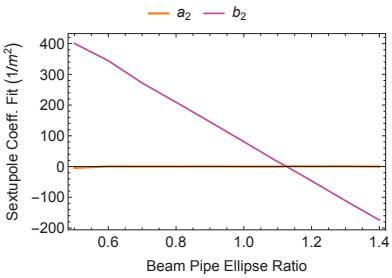

Figure 4: Sextupole coefficients a_2 and b_2 versus beam pipe ellipse shape.

ELLIPTICAL CAVITY

Subsequently we optimized an elliptical cavity, shown in Fig. 2. First we made the the beam pipe cylindrical with 4 cm diameter and optimized the ellipse aspect ratio of the cavity to maximize the spacing between the accelerating, working deflecting, and parasitic deflecting fields. The results are shown in Fig. 3. For further optimization we set the ellipse aspect ratio to be 1.2. Then we made the beam pipe elliptical, maintaining a 4 cm aperture on the horizontal plane in order to minimize the sextupole component. At beam pipe ellipse aspect ratio of 1.12 the sextupole component is minimal. The results are shown in Fig. 4. The final cavity is shown in Fig. 2.

The optimal shape of the elliptical crab cavity was assembled with the input, LOM, and HOM couplers as shown

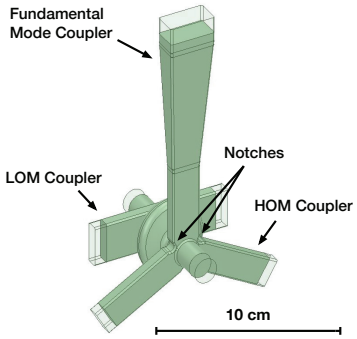

Figure 5: Elliptical crab cavity with the input, LOM, and HOM couplers.

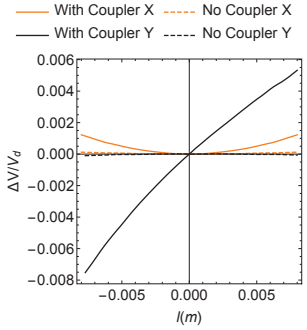

(a) Kick variation in x and y, comparison with and without the couplers.

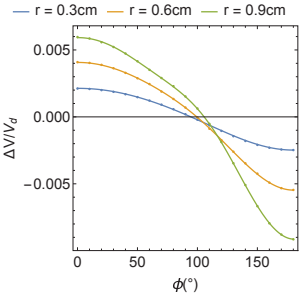

(b) Kick variation in the azimuth at different radius. Dotted line is simulation data, solid line is multipole fit.

Figure 6: Kick variation for the elliptical crab cavity with the couplers.

in Fig. 5. We followed one of the APS coupler configurations [16], having a two-port LOM waveguide connected to the front of the cavity, and three HOM waveguides in a Y shape from the back. The LOM waveguide cutoff is approximately 2.1 GHz, slightly below the frequency of the monopole mode. The dimensions of the LOM waveguide were optimized to minimize the loaded quality factor of the monopole mode. The HOM waveguide cutoff is approximately 3.0 GHz, in-between the frequencies of the working and parasitic dipole modes. The power coupling waveguide is connected to one of the three HOM waveguides through a taper. The length of this transition was optimized to obtain the desired total quality factor of the target dipole mode. Notches were added in the HOM as shown in Fig. 5 to eliminate a mode that was trapped there.

Table 2: Lowest Order Modes in the 6$^{\text{th}}$ Harmonic Cavity with Input, LOM, and HOM Couplers

Mode	Frequency	Loaded Q Factor
Monopole	2.12 GHz	417
Working Dipole	2.858 GHz	2×10^6
Parasitic Dipole	3.12 GHz	178

Table 2 summarizes the frequencies and quality factors of the three lowest order modes. We were not able to further reduce the quality factor of the monopole mode. Table 3 summarizes the achieved parameters of the cavity. The longitudinal and transverse wake impedances were calculated using the resonator approximation [22] from the HFSS eigenmode data. The longitudinal wake impedance is substantially higher than the specification, but similar to the values APS reported in [15]. We can potentially accept this high value if we use a longitudinal bunch-by-bunch feedback system. The y transverse wake impedance is extremely high, similar to the APS design [15], which is expected since this is a superconducting cavity. Fig. 6a and Fig. 6b show the kick variation with x and y and azimuthally for different radius having multipole fields of order $n = 1, 2, 3, 4, 5$. Even with the coupler, the sextupole component is within the specifications. The coupler also induces a quadrupole-like component in the y-direction.

CONCLUSION

In this work we explored two superconducting crab cavity options for short X-ray pulse production in SPEAR3. One was the single-cell QMiR cavity. We found that with this shape we cannot meet our field uniformity specifications due to higher order multipole fields. Then we optimized a traditional elliptical cavity with the input, LOM, and HOM couplers following the APS design. The longitudinal wake impedance is substantially higher than the specification, but we can potentially mitigate this issue using a longitudinal bunch-by-bunch feedback system. The sextupole component meets our specifications. The input coupler induces a quadrupole component, the effect of which we will investigate in future work.

ACKNOWLEDGMENTS

The authors wish to thank James Safranek and Jim Sebek for the fruitful conversations.

Table 3: Parameters for the 6$^{\text{th}}$ Harmonic Cavity

Parameter	Value
Frequency f_1	2.858 GHz
Beam aperture horizontal width d_x	4 cm
Intrinsic quality factor Q_0	1×10^9
Total quality factor Q_t	2×10^6
Resistive losses for 0.5 MV kick	5.7 W
Power for 0.5 MV kick	2.9 kW
Kick impedance R_t	87.3 MΩ
R_t/Q	43.65 Ω
Peak surface E-field for 0.5 MV kick	39 MV m^{-1}
Peak surface B-field for 0.5 MV kick	100 mT
Sextupole field K_2L	0.03 m^{-1}
Monopole impedance @ 2.12 GHz	46.8 kΩ
Dipole wake impedance x	0.45 MΩ m^{-1}
Dipole wake impedance y	5.3 GΩ m^{-1}

REFERENCES

[1] H. Winick, "Fourth Generation Light Sources," in *Proc. 17th Particle Accelerator Conf. (PAC'97)*, Vancouver, Canada, May 1997, paper FBC003, pp. 37–41.

[2] M. E. Couprie, "New generation of light sources: Present and future," *Journal of Electron Spectroscopy and Related Phenomena*, vol. 196, pp. 3–13, Oct. 2014.

[3] T. C. B. Harlang, Y. Liu, O. Gordivska, L. A. Fredin, C. S. Ponseca, P. Huang, P. Chábera, K. S. Kjær, H. Mateos, J. Uhlig, R. Lomoth, R. Wallenberg, S. Styring, P. Persson, V. Sundström, and K. Wärnmark, "Iron sensitizer converts light to electrons with 92% yield," *Nature Chemistry*, vol. 7, no. 11, pp. 883–889, 2015.

[4] J. J. Choi and S. J. L. Billinge, "Perovskites at the nanoscale: from fundamentals to applications," *Nanoscale*, vol. 8, pp. 6206–6208, 2016.

[5] H. Zhu, K. Miyata, Y. Fu, J. Wang, P. P. Joshi, D. Niesner, K. W. Williams, S. Jin, and X. Y. Zhu, "Screening in crystalline liquids protects energetic carriers in hybrid perovskites," *Science*, vol. 353, no. 6306, pp. 1409–1413, 2016.

[6] W. Zhang, K. S. Kjær, R. Alonso-Mori, U. Bergmann, M. Chollet, L. A. Fredin, R. G. Hadt, R. W. Hartsock, T. Harlang, T. Kroll, K. Kubiček, H. T. Lemke, H. W. Liang, Y. Liu, M. M. Nielsen, P. Persson, J. S. Robinson, E. I. Solomon, Z. Sun, D. Sokaras, T. B. van Driel, T.-C. Weng, D. Zhu, K. Wärnmark, V. Sundström, and K. J. Gaffney, "Manipulating charge transfer excited state relaxation and spin crossover in iron coordination complexes with ligand substitution," *Chem. Sci.*, vol. 8, pp. 515–523, 2017.

[7] J. A. Johnson, A. A. Maznev, J. Cuffe, J. K. Eliason, A. J. Minnich, T. Kehoe, C. M. S. Torres, G. Chen, and K. A. Nelson, "Direct Measurement of Room-Temperature Nondiffusive Thermal Transport Over Micron Distances in a Silicon Membrane," *Phys. Rev. Lett.*, vol. 110, p. 025901, Jan. 2013.

[8] K. Haldrup, G. Vankó, W. Gawelda, A. Galler, G. Doumy, A. M. March, E. P. Kanter, A. Bordage, A. Dohn, T. B. van Driel, K. S. Kjær, H. T. Lemke, S. E. Canton, J. Uhlig, V. Sundström, L. Young, S. H. Southworth, M. M. Nielsen, and C. Bressler, "Guest–Host Interactions Investigated by Time-Resolved X-ray Spectroscopies and Scattering at MHz Rates: Solvation Dynamics and Photoinduced Spin Transition in Aqueous Fe(bipy)32+," *The Journal of Physical Chemistry A*, vol. 116, no. 40, pp. 9878–9887, 2012.

[9] C. Sun, D. S. Robin, C. Steier, and G. Portmann, "Characterization of pseudosingle bunch kick-and-cancel operational mode," *Phys. Rev. ST Accel. Beams*, vol. 18, p. 120702, Dec. 2015.

[10] W. Guo, B. Yang, C. x. Wang, K. Harkay, and M. Borland, "Generating picosecond x-ray pulses in synchrotron light sources using dipole kickers," *Phys. Rev. ST Accel. Beams*, vol. 10, p. 020701, Feb. 2007.

[11] X. Huang, T. Rabedeau, and J. Safranek, "Generation of picosecond electron bunches in storage rings," *Journal of Synchrotron Radiation*, vol. 21, no. 5, pp. 961–967, Sep. 2014.

[12] X. Huang, J. Safranek, and K. Bane, "Injecting short pulses into SPEAR3," Tech. Rep., 2015.

[13] A. Zholents, P. Heimann, M. Zolotorev, and J. Byrd, "Generation of subpicosecond X-ray pulses using RF orbit deflection," *Nuclear Instruments and Methods in Physics Research Section A: Accelerators, Spectrometers, Detectors and Associated Equipment*, vol. 425, no. 1, pp. 385–389, 1999.

[14] M. Borland, "Simulation and analysis of using deflecting cavities to produce short x-ray pulses with the Advanced Photon Source," *Phys. Rev. ST Accel. Beams*, vol. 8, p. 074001, Jul. 2005.

[15] H. Wang *et al.*, "Crab Cavity and Cryomodule Prototype Development for the Advanced Photon Source," in *Proc. 24th Particle Accelerator Conf. (PAC'11)*, New York, NY, USA, Mar.-Apr. 2011, paper WEOCS7, pp. 1472–1474.

[16] R. Nassiri *et al.*, "Status of the Short-Pulse X-ray Project (SPX) at the Advanced Photon Source (APS)," in *Proc. 24th Particle Accelerator Conf. (PAC'11)*, New York, NY, USA, Mar.-Apr. 2011, paper WEOBS5, pp. 1427–1429.

[17] G. J. Waldschmidt *et al.*, "Superconducting Cavity Design for Short-Pulse X-Rays at the Advanced Photon Source," in *Proc. 24th Particle Accelerator Conf. (PAC'11)*, New York, NY, USA, Mar.-Apr. 2011, paper THP212, pp. 2516–2518.

[18] L. Xiao, Z. Li, C.-K. Ng, A. Nassiri, G. J. Waldschmidt, G. Wu, R. A. Rimmer, and H. Wang, "Higher Order Modes Damping Analysis for the SPX Deflecting Cavity Cryomodule," Tech. Rep., 2012.

[19] J. K. G. Wuestefeld, A. Jankowiak and M. Ries, "Simultaneous Long and Short Electron Bunches in the BESSY II Storage Ring," in *Proc. 2nd Int. Particle Accelerator Conf. (IPAC'11)*, San Sebastian, Spain, Sep. 2011, paper THPC014, pp. 2936–2938.

[20] Z. Li *et al.*, "Normal Conducting CW Transverse Crab Cavity For Producing Short Pulses In SPEAR3," in *Proc. 8th Int. Particle Accelerator Conf. (IPAC'17)*, Copenhagen, Denmark, May 2017, paper WEPAB115, pp. 2840–2843.

[21] A. Lunin, I. Gonin, M. Awida, T. Khabiboulline, V. Yakovlev, and A. Zholents, "Design of a Quasi-waveguide Multicell Deflecting Cavity for the Advanced Photon Source," *Physics Procedia*, vol. 79, pp. 54–62, 2015.

[22] K. Semyon and Z. Bruno, *Impedances and Wakes in High Energy Particle Accelerators*. World Scientific, 1998.